Protein kinase C α is a central signaling node and therapeutic target for breast cancer stem cells

Wai Leong Tam[1,8], **Haihui Lu**[1], **Joyce Buikhuisen**[1], **Boon Seng Soh**[2], **Elgene Lim**[3], **Ferenc Reinhardt**[1], **Zhenhua Jeremy Wu**[4], **Jordan A. Krall**[1], **Brian Bierie**[1], **Wenjun Guo**[5], **Xi Chen**[6], **Xiaole Shirley Liu**[4], **Myles Brown**[3], **Bing Lim**[2], and **Robert A. Weinberg**[1,7,8,#]

[1]Whitehead Institute for Biomedical Research, Cambridge, MA 02142, USA

[2]Genome Institute of Singapore, 60 Biopolis Street, 138672, Singapore

[3]Dana-Farber Cancer Institute and Harvard Medical School, Boston, MA 02215, USA

[4]Dana Farber Cancer Institute and Harvard School of Public Health, Boston, MA 02115, USA

[5]Gottesman Institute for Stem Cell and Regenerative Medicine Research, Albert Einstein College of Medicine, Bronx, NY 10461, USA

[6]Weill Cornell Medical College, New York, NY 10065, USA

[7]Department of Biology, Massachusetts Institute of Technology, Cambridge, MA 02142, USA

[8]MIT Ludwig Center for Molecular Oncology, Cambridge, MA 02139, USA

SUMMARY

The epithelial-mesenchymal transition program becomes activated during malignant progression and can enrich for cancer stem cells (CSCs). We report that inhibition of protein kinase C α (PKCα) specifically targets CSCs, but has little effect on non-CSCs. The formation of CSCs from non-stem cells involves a shift from EGFR to PDGFR signaling, and results in the PKCα-dependent activation of FRA1. We identified an AP-1 molecular switch in which c-FOS and FRA1 are preferentially utilized in non-CSCs and CSCs, respectively. PKCα and FRA1 expression is associated with the aggressive triple-negative breast cancers and the depletion of FRA1 results in a mesenchymal-epithelial transition. Hence, identifying molecular features that shift between cell states can be exploited to target signaling components critical to CSCs.

#Correspondence: weinberg@wi.mit.edu (R.A.W.).

INTRODUCTION

Cancer stem cells (CSCs), which are defined by their tumor-initiating properties, have been identified within breast, colon, head and neck, lung and prostate carcinomas (Ailles and Weissman, 2007). These cells appear to be responsible for driving tumor growth, recurrence and metastasis (Al-Hajj et al., 2003; Dalerba et al., 2007). In experimental models of cancer development, treatment of bulk cancer cell populations within tumors or cancer cell lines propagated in culture with chemo- or radiotherapy has been shown to select for the outgrowth of therapy-resistant subpopulations of cancer cells that are more tumorigenic, invasive and stem-like (Creighton et al., 2009; Gupta et al., 2009). Hence, cancer therapies may be rendered ineffective because the bulk of cancer cells within a tumor may be eliminated while leaving behind CSC-enriched cells that proceed to regenerate tumors. These tumors are often more malignant than was observed prior to treatment underscoring the need for a detailed understanding of the molecular differences between CSCs and non-CSCs to discover and exploit cell state-specific features that may render CSCs susceptible to selective therapeutic intervention.

Numerous studies have used existing cancer cell lines to identify compounds that target cells bearing specific gene mutations or exhibiting a more malignant phenotype; these studies did not, however, address the specific effects of certain treatments on CSCs because the representation of CSCs within these cell lines was poorly defined. In the case of breast cancer, several markers, including $CD44^{hi}/CD24^{lo}$, aldehyde dehydrogenase ($ALDH1^{+}$), Hoechst dye efflux, and the retention of the PKH26 lipophilic dye, have been shown to enrich for CSCs in various cell lines (Al-Hajj et al., 2003; Ginestier et al., 2007; Pece et al., 2010). However, regardless of the enrichment procedure, these initially purified cells with CSC properties often differentiate rapidly into cells exhibiting a non-CSC profile, making it difficult to identify cell state-specific inhibitors *in vitro*.

CSCs are generated in some and perhaps all carcinomas as one of the products of an epithelial-mesenchymal transition (EMT), indicating that these cells possess a more mesenchymal phenotype that is associated with highly aggressive traits (Nieto, 2011; Thiery et al., 2009). We undertook to develop a method by which we could clearly distinguish chemical inhibitors that target breast CSCs from those that affect non-CSCs. Within normal mammary epithelial cells (MECs), the forced expression of EMT-inducing transcription factors (EMT-TFs) endows cells with mesenchymal traits accompanied by the loss of epithelial markers. These cells were shown to possess enhanced stem cell activity *in vitro* and *in vivo* (Mani et al., 2008; Morel et al., 2008). Likewise, in populations of weakly or non-tumorigenic breast cancer cells, passage through the EMT program dramatically increases CSC frequency along with the acquisition of mesenchymal properties that include a distinctive $CD44^{hi}/CD24^{lo}$ cell-surface marker profile, mammosphere-forming ability, heightened resistance to chemotherapeutics, and increased tumor-initiating ability (Nieto, 2011; Thiery et al., 2009).

In the present work, we took a directed approach to discover key regulatory genes unique to the mesenchymal state whose expression is elevated in CSCs.

RESULTS

Identification of kinases expressed differentially in EMT-induced cells

To understand the molecular changes associated with epithelial cells that have passed through an EMT, we transduced genes encoding the Twist, Snail and Slug EMT-TFs into HMLE human MECs that had previously been immortalized through the introduction of the hTERT and SV40 early-region genes (Mani et al., 2008). As anticipated, the resulting cells (HMLE-Twist, HMLE-Snail and HMLE-Slug) displayed a set of mesenchymal markers and were judged by these criteria to have undergone an EMT (Figures 1A and S1A). These cells were predominantly CD44^{hi}/CD24^{lo} (data not shown) and formed mammospheres more efficiently than the parental epithelial cells (Figure 1B), indicating they were enriched for stem cell activity.

Using microarray gene expression analyses, we searched for kinase-encoding genes that exhibited the greatest differences in expression in the EMT-TF-induced mesenchymal cells relative to the parental HMLE cells. A group of kinase-encoding genes were overexpressed at least two fold in HMLE-Twist, HMLE-Snail and HMLE-Slug cells relative to the HMLE population (Figure 1C and Table S1). Several of these genes, including *CLK1*, *EPHA2*, *NME7*, *PRKCA* (hereafter referred as *PKCα*), *SGK1*, *SPHK1* and *CDK6*, have been reported to promote cancer cell invasion and motility but were not previously implicated either as components of the EMT transcription program or in the maintenance of mesenchymal and CSC states. We validated the expression of the top selected kinase mRNAs by quantitative PCR (Figure S1B).

The changes in the expression patterns of these kinases during the EMT suggested an opportunity for selective therapeutic intervention using kinase inhibitors. We wished to develop an assay that could be used to determine whether any of the upregulated kinases could be pharmacologically targeted to preferentially kill the mesenchymal cells. Because the mesenchymal cells analyzed above carried constitutively expressed EMT-TFs and were therefore locked in the mesenchymal state, we reasoned their response to chemical inhibitors might not be representative of mesenchymal cells that arise *in vivo* through the physiological and presumably reversible upregulation of endogenous EMT-TFs, limiting the utility of the EMT-TF vector-transduced cells in chemical inhibitor screens.

Therefore, we derived populations of HMLE cells that had spontaneously undergone an EMT and stably resided thereafter in a mesenchymal state (Figure 1D). Hence, their phenotypic state was governed by endogenously expressed EMT-TFs. We derived 11 such lines, termed Naturally Arising MEsenchymal Cells (NAMECs), from bulk cultures of HMLE cells. We found that NAMECs expressed elevated levels of endogenous EMT-TFs (Twist, Snail, Slug and Zeb1) and associated markers (vimentin, N-cadherin and fibronectin) as well as loss of the key epithelial adherens junction protein, E-cadherin (encoded by *CDH1*) (Figures 1E, 1F, S1A and S1C). Similar to EMT-TF-induced cells and the resident mammary epithelial stem cells that are naturally present within HMLE populations, NAMECs were also predominately CD44^{hi}/CD24^{lo} (Figure 1G). They exhibited an 11.3-fold higher mammosphere-forming ability relative to HMLE cells (Figure 1H). Thus,

NAMECs exhibited characteristics of cells that have passed through an EMT and differed greatly from parental HMLE cells.

Depletion of stem-like cells by select kinase inhibitors

To identify kinase inhibitors that selectively targeted mesenchymal-like cells bearing stem cell properties, we established a screen that measured the ability of candidate inhibitors to preferentially deplete mesenchymal NAMECs but not HMLE cells. We labeled one of the NAMEC lines (NAMEC8) with the tdTomato red fluorescent protein (NAMEC-Tom) and the HMLE cells with green fluorescent protein (HMLE-GFP). We then attempted to reconstitute certain stem cell and non-stem cell interactions that might operate *in vivo* by mixing the two cell populations in culture in a 5:1 ratio (Figures 2A and S2A). We then challenged these cultures with a panel of kinase inhibitors. We initially targeted several proteins kinases that were elevated in HMLE-Twist, HMLE-Snail, HMLE-Slug cells and NAMECs relative to HMLE using of a panel of 15 commercially available kinase inhibitors (Figures 1C, S1B and S2B). Figure 2B illustrates their effects on the proportion of surviving NAMEC-Tom and HMLE-GFP cells at the end of a six-day treatment period and the numbers of viable cells were quantified with flow cytometry to determine the fraction of NAMEC-Tom or HMLE-GFP cells in inhibitor-treated populations relative to vehicle-treated controls.

The four inhibitors targeting PKCα (PKC 20-28, Ro-31-8220, Ro-32-0432 and bisindolylmaleimide I) showed a 6.8- to 12.1-fold lower LC_{50} (lethal concentration, 50%) against NAMEC-Tom cells relative to HMLE-GFP cells (Figures 2C and 2D). These findings were validated in three other NAMEC cell lines (Figures S2C and S2D). Since PKCα was also elevated in $CD44^{hi}/CD24^{lo}$ HMLE cells (Figure 2E), we tested whether these stem-like cells were sensitive to the inhibitors. Indeed, treatment of bulk HMLE cells with two different PKCα inhibitors reduced the $CD44^{hi}/CD24^{lo}$ cell compartment whereas the $CD44^{lo}/CD24^{hi}$ population remained unaffected (Figure S2E).

While total and phosphorylated PKCα were overexpressed in a variety of derived mesenchymal cells (Figure S2F), the phosphorylation status of PKCα is constitutive and not a useful indicator of its activity (Newton, 2001). Furthermore, active site inhibitors, such as bisindolylmaleimide, could paradoxically stabilize phosphorylated PKC (Cameron et al., 2009; Gould et al., 2011). Accordingly, we validated PKC enzymatic activity in these cells and found that the derived mesenchymal cells possessed on average 8.5-fold higher levels of total PKC activity relative to HMLE cells (Figure 2F).

The inhibitors targeting PKCη, CLK1, CDK6 and JAK1 also appeared to deplete NAMEC-Tom cells preferentially (Figure 2B). However, these agents were not included in subsequent studies as only a single inhibitor was available against each of these kinases, preventing us from controlling for possible off-target effects. In stark contrast to the effect of the pathway-specific inhibitors, three non pathway-specific compounds, staurosporine, doxorubicin and paclitaxel preferentially depleted HMLE-GFP cells instead (Figures 2B and 2D). This supported previous observations that non cell state-specific inhibitors can enhance the representation of more aggressive cancer stem-like cells within heterogeneous cell populations following treatment (Creighton et al., 2009; Gupta et al., 2009).

To determine how PKCα inhibitors affected these more susceptible cell populations, we tested whether they induced apoptosis. The mixed cell populations were treated with Ro-31-8220 for three days and 89.4% of NAMEC-Tom cells underwent apoptosis in comparison to 22.4% of the HMLE-GFP cells (Figure 2G). Conversely, paclitaxel and staurosporine resulted in HMLE-GFP cell apoptosis, leaving NAMEC-Tom cells less affected.

As it remained possible that the four PKCα inhibitors used in our analyses acted in an off-target manner, we depleted PKCα with shRNA (Figure 2H). Mixed NAMEC-Tom and HMLE-GFP cultures were infected with lentiviral shRNAs targeting PKCα and then seeded separately, after sorting for either Tom[+] or GFP[+] expression. Consistent with the use of chemical inhibitors, depletion of PKCα resulted in the substantial loss of NAMECs whereas HMLE cells were less affected (Figure 2I). These observations confirmed the greater dependence on PKCα-regulated signaling networks in cells that have passed through an EMT program.

Conservation of cell state-specific features upon oncogenic transformation

To test whether neoplastic cells that have passed through an EMT program acquire a greater potential to generate CSCs, we ectopically expressed comparable levels of H-RAS[G12V] in NAMECs and HMLE cells (Figure 3A). As few as 500 of the resulting NAMEC-RAS cells, when implanted into NOD-SCID mice, were sufficient for tumor-initiation in six out of 10 hosts, whereas as many as 25,000 of the corresponding HMLE-RAS cells failed to form tumors (Figure 3A). Based on a limiting dilution assay, the frequency of CSCs was calculated to be approximately 1/2314 for NAMEC-RAS and 1/463783 for HMLE-RAS cells. Thus, transformation of preneoplastic stem cells expressing mesenchymal traits gave rise to CSCs far more efficiently than bulk epithelial cells.

To investigate whether PKCα inhibition would also preferentially affect CSC-enriched NAMEC-RAS cells, we first determined if *PKCα* mRNA levels remained differentially regulated between NAMEC-RAS and HMLE-RAS cell populations. We found that the mRNA levels of *PKCα* and other kinase-encoding genes that were examined previously remained higher in NAMEC-RAS cells compared to the HMLE-RAS cells; this echoed the behavior of EMT-TF-induced mesenchymal cells that had been transduced with the *RAS[G12V]* vector (Figure 3B). We then mixed NAMEC-RAS cells labeled with tdTomato (NAMEC-Tom-RAS) and HMLE-RAS cells labeled with GFP (HMLE-GFP-RAS) and re-tested the effects of kinase inhibition and found that NAMEC-Tom-RAS cells were more sensitive to PKCα inhibition relative to HMLE-GFP-RAS cells (Figure 3C). In contrast, NAMEC-Tom-RAS cells were more resistant to paclitaxel and staurosporine than HMLE-GFP-RAS cells (Figure 3C). When these various transformed cell populations were implanted into NOD-SCID mice, NAMEC-RAS-derived tumors continued to express PKCα but HMLE-RAS tumors did not (Figure 3D).

To assess the therapeutic utility of PKCα inhibitors, NAMEC-RAS cells were implanted in NOD-SCID mice and treated for 30 days with a daily intraperitoneal dose of either a PKCα inhibitor (Ro-31-8220) or a DMSO solvent control; additional control animals were left untreated. These dosages were well-tolerated in mice and had no adverse effects after 30

days of treatment followed by eight weeks of observation. Significant tumor burdens were observed after 15 weeks in all control-treated mice whereas only four of eight mice treated with PKCα inhibitor formed tumors (Figure 3E). Hence, PKCα inhibition reduced tumor-initiating frequency and tumor growth of the CSC-enriched populations *in vivo*. We also examined whether PKCα inhibition would have any effect on the growth of already-established tumors. Xenografted NAMEC-RAS tumors were allowed to reach approximately 2 mm in diameter (assessed by palpation) four weeks after implantation and then exposed to treatments. Tumors from control-treated mice reached ~1.03 g six weeks later, whereas those from PKCα inhibitor-treated mice only weighed ~0.25 g (Figure 3F). These results demonstrated the therapeutic effects of PKCα inhibition on the continued growth of already-established tumors.

A switch from EGFR to PDGFR signaling is induced upon EMT

The greater reliance of CSCs on PKCα led us to question whether cells that have passed through an EMT respond to mitogenic and trophic signals differently from those that have not. We attempted to trace the sources of the upstream signals that might be responsible for activating PKCα and postulated that certain receptor tyrosine kinases induced by the EMT program might be involved. We speculated that the EGF receptor (EGFR) might activate PKCα in cells that had undergone an EMT, because EGFR overexpression and amplification are positively associated with breast cancer progression (Carey et al., 2010). However, in mesenchymal cell populations, the expression of endogenous total and phosphorylated EGFR^{Y1068} was reduced relative to HMLE cells (Figure 4A). Treatment of co-mixed NAMEC-RAS-Tom and HMLE-RAS-GFP cells with either of two EGFR inhibitors preferentially selected against HMLE-RAS-GFP cells (Figure 4B). Hence, the more epithelial, non-CSC-enriched populations depended more strongly upon sustained EGFR signaling than the mesenchymal CSC-enriched cell populations.

We used proteome analysis to identify potential RTKs associated with an EMT and responsible for the activation of PKCα. The most differentially expressed RTK, exhibiting a 13-fold increase in representative peptides in HMLE-Twist cells relative to HMLE cells, was PDGFRβ (encoded by *PDGFRB*) (data not shown). In addition, mRNAs of *PDGFRA* (encoding PDGFRα) and *PDGFRB*, as well as their ligand *PDGFC*, were highly expressed in basal B subtype of breast cancer cell lines bearing mesenchymal properties, but not in luminal-like cell counterparts bearing more epithelial features (Figure 4C). *PKCα* mRNA was also highly expressed in basal B, and not luminal-like, breast cancer cells (Figure 4C). This is consistent with the notion that basal-like tumors contain cells that behave as if they have undergone at least a partial EMT (Blick et al., 2008; Sarrio et al., 2008).

To determine whether PDGF autocrine signaling might be activated following an EMT, we surveyed the expression of PDGFR ligands in the mesenchymal and epithelial cell populations. *PDGFA*, *PDGFB* and *PDGFD* mRNAs were not expressed in either cell state (data not shown), indicating that only PDGFC could participate in such autocrine signaling. In mesenchymal cell populations, *PDGFC* mRNA was indeed upregulated (Figure 4D); total and phosphorylated PDGFRα/β proteins were also induced in these cells (Figure 4E).

Additionally, *PDGFRA*, *PDGFRB* and *PDGFC* mRNAs were upregulated specifically in the CD44^{hi}/CD24^{lo} stem cell-enriched subpopulation (Figure S3A).

We also monitored the activity of PDGFR in the mesenchymal cell populations. Culturing NAMECs for 24 hr in serum-free, growth factor-depleted medium reduced phosphorylation of PDGFRβ modestly relative to NAMECs maintained in complete medium, whereas application of either a PDGFR-neutralizing antibody or a PDGFR pharmacologic inhibitor led to a 4.3- and 6.8-fold reduction, respectively, in p-PDGFRβ^{Y751} (Figure 4F). Conversely, the exposure of the growth factor-depleted NAMECs to PDGFC resulted in increased phosphorylation of PDGFRβ (Figure 4F), while HMLE cells showed no response to PDGFC (data not shown). This provided further support for the specific activation of autocrine PDGF signaling activity following induction EMT.

Levels of phospholipase C γ 1 and 2 (PLCγ1 and PLCγ2) proteins, which are known to transduce signals from PDGFRα/β to PKCα (Rhee, 2001), were also elevated in the EMT TF-transduced and NAMEC cells (Figure 4E). To examine whether PLCγ was activated by PDGFR, NAMECs were treated with either of two PDGFR inhibitors (PDGFR Inh III and PDGFR Inh IV). Levels of the two p-PLCγ1^{Y783} and p-PLCγ2^{Y1217} activated forms were reduced, whereas total PLCγ1 and PLCγ2 protein levels remained unaltered (Figure S3B). We next sought to determine whether PKCα activation was dependent on the observed activations of PDGFR and PLCγ, the latter activates PKCα through its production of diacylglycerol (Saito et al., 2002). Exposure of NAMECs to a PLCγ inhibitor (U73122) reduced total PKC enzymatic activity (Figure S3C). Likewise, pharmacologic inhibition of PDGFR in NAMECs reduced PKC activity (Figure S3C). Together, these results confirmed that PKCα activity operated downstream of PDGFR and depended on the actions of PLCγ.

Since PDGF autocrine signaling was activated in cells that had undergone an EMT, we reasoned that this might be important for their survival and that the inhibition of PDGFR could be useful for the selective killing of CSCs. Co-mixed NAMEC-Tom-RAS and HMLE-GFP-RAS cells were treated with each of these inhibitors and NAMEC-Tom-RAS cells exhibited a 3.2–3.8 fold lower LC$_{50}$ for the PDGFR inhibitors tested relative to HMLE-GFP-RAS cells (Figure 4G). It thus appeared that the EMT, along with the acquisition of CSC-like traits, was accompanied by a downregulation of EGFR and concomitant upregulation of PDGFR, highlighting the preferential utilization of different signaling networks in different cellular states. We noted that a pharmacologic inhibitor that is completely specific to inhibition of PDGFRα/β is currently unavailable and the two PDGFRα/β inhibitors used here cross-inhibited c-KIT- and VEGFR-associated tyrosine kinases.

Cell-state dependent utilization of c-FOS or FRA1 during EMT

We sought to elucidate the mechanism(s) through which PKCα acts to support the mesenchymal cell state and to identify downstream mediators of PKCα in cells that have undergone an EMT. We surveyed for PKCα substrates identified by others in various cellular contexts (Abate et al., 1991; Gruda et al., 1994; Kang et al., 2012) and focused on those upregulated together with PKCα expression during an EMT (Figure S4A). Among genes examined, *FOSL1* mRNA (encoding the FRA1 protein) was the most upregulated

target of PKCα in the HMLE-Twist, HMLE-Snail and HMLE-Slug cells. This prompted us to further examine the connection between PKCα and FRA1. Of note, we could not exclude the possible functional importance of other genes encoding PKCα substrates that were not transcriptionally upregulated.

FRA1 is a member of the FOS family of transcription factors that when phosphorylated downstream of PKCα signaling associate with members of the JUN family of transcription factors to form heterodimeric activator protein-1 (AP-1) complexes to transcriptionally regulate target gene expression (Abate et al., 1991). To confirm that FRA1 operated downstream of PKCα, NAMECs were treated with either of two PKCα inhibitors. Levels of p-FRA1^{S265} were strongly downregulated whereas total FRA1 levels remained unchanged, indicating that FRA1 phosphorylation was indeed dependent on PKCα activity (Figure 5A).

We speculated that c-JUN (encoded by *JUN*) was a binding partner of FRA1 as our previous work demonstrated induction of c-JUN during passage through an EMT (Scheel et al., 2011). Indeed, we found that total and phospho-c-JUN^{S63} as well as the Jun N-terminal kinase (JNK), which is required for the activation of c-JUN, were upregulated in mesenchymal cell populations (Figures 5B and S4B). Other JUN family members, JUNB and JUND, did not exhibit consistent up- or down-regulation following passage through EMT, indicating that their expression was not cell-state dependent. Unexpectedly, c-FOS (encoded by *FOS*), which has been extensively documented as a partner of c-JUN (Eferl and Wagner, 2003), was downregulated during passage through an EMT (Figures 5B and S4B). Total and phospho-FRA1^{S265} levels, by contrast, were increased. Hence, epithelial and mesenchymal cells appeared capable of assembling AP-1 complexes, but of quite different composition, in that FRA1 seemed to replace c-FOS as the partner of JUN following passage through an EMT.

We sought to understand the functional significance of the c-FOS-FRA1 molecular switch during the EMT. Knockdown of FRA1 with two independent shRNAs preferentially reduced NAMEC-Tom cell numbers but had a lesser impact on HMLE-GFP cells (Figures 5C and S4C). In contrast, HMLE-GFP cells were preferentially depleted upon c-FOS knockdown while NAMEC-Tom cells were significantly less affected. This highlighted the cell-state specific dependence on either c-FOS or FRA1 for maintaining cell viability (Figure 5C). We performed co-immunoprecipitation experiments to validate the formation of AP-1 complexes and the nature of their constituent subunits. In NAMECs, immunoprecipitation of FRA1 showed physical association with c-JUN, JUNB and JUND (Figure 5D). In a reciprocal manner, pull-down of c-JUN demonstrated its interaction with FRA1 but not c-FOS (Figure 5D). The converse pattern was observed in HMLE cells, in which c-FOS strongly associated with JUNB and JUND but not c-JUN, which was downregulated in the epithelial state (Figure 5D). Furthermore, chromatin immunoprecipitation analyses revealed c-FOS binding to the promoters of genes encoding E-cadherin and Crumb3, two key epithelial proteins, in HMLE cells. The same promoters, however, were not bound by FRA1 in NAMECs, which did not express either protein (Figure 5E). Hence, during execution of the EMT program, there is a switch from the use of c-FOS to FRA1 as the preferred component of AP-1 transcription factor complexes.

Control of FRA1 activation by ERK signaling

We sought to uncover additional downstream targets of PKCα beyond FRA1 that might be crucial for supporting the EMT program. c-Raf is another substrate of PKCα that sustains activation of ERK signaling and helps to promote mesenchymal cell phenotypes (Kolch et al., 1993). Examination of proteins involved in the ERK pathway revealed increased expression of both total and phosphorylated levels of B-RAF, c-RAF and ERK1/2 in the mesenchymal cell populations (Figure 5F).

As ERK signaling is commonly controlled by RAS activity, we tested whether mesenchymal cells contained higher RAS expression or activated RAS than did epithelial cells. Interestingly, levels of total RAS and activated GTP-bound RAS were similar among epithelial and mesenchymal cell types (Figures 5F and 5G). This led us to propose that the enhanced ERK signaling in the mesenchymal cell state was primarily mediated by PKCα signaling, rather than through the RAS-RAF pathway. To test this notion, we exposed NAMECs to PKCα inhibitors and found reduced p-c-RAF, p-MEK1/2 and p-ERK1/2 levels (Figures 5H and S4D). Inhibitors of PDGFR signaling, likewise, blunted ERK signaling as indicated by decreased p-c-RAF, p-MEK1/2 and p-ERK1/2 levels (Figure S4E). Hence, enhanced activity of ERK signaling during EMT was conferred in part by signaling through PDGFR and PKCα.

FRA1, which we showed earlier to be downstream of PKCα, has also been reported to serve as a direct substrate of p-ERK1/2 (Kakumoto et al., 2006). Thus we speculated that the increased p-FRA1 activity in the mesenchymal cells could be further augmented by elevated ERK signaling. Accordingly, blockade of ERK1/2 phosphorylation with a MEK inhibitor in NAMECs decreased p-FRA1 levels but did not affect the levels of total FRA1 or p-c-JUN (Figure 5I), confirming that ERK1/2 signaling promoted the phosphorylation of FRA1. Together, these observations indicate that PKCα signaling in mesenchymal cells leads to activation of FRA1, downstream of both PKCα and ERK1/2.

Role of FRA1 in tumor initiation by breast cancer cells

We sought to understand whether FRA1 might be functionally important for the subset of human breast cancer cells that exhibit mesenchymal traits. Accordingly, we depleted FRA1 by RNAi in two basal-like (basal B) breast cancer cell lines, MDA-MB-231 and SUM159, both of which do not express HER2, estrogen receptor (ER), or progesterone receptor (PR). In both cell lines, FRA1 depletion resulted in a morphologic response resembling a mesenchymal-epithelial transition (MET), in which otherwise mesenchymal-like cancer cells formed cobblestone sheets resembling those assembled by epithelial cells (Figure 6A). The loss of *VIM*, *FN1* and *CDH2* mRNA expression accompanied by the gain of *CDH1* mRNA expression was observed (Figure 6B). Moreover, in both cell lines depleted of FRA1, *FOS* mRNA expression, which we had previously associated with the epithelial cell phenotype, was strikingly increased (Figure 6C).

FRA1 knockdown did not significantly affect proliferation of MDA-MB-231 or SUM159 cells *in vitro* (Figure S5A). However, FRA1-depleted cells formed tumors with a reduced frequency and were substantially smaller size relative to shRNA controls when xenografted

into female NOD-SCID mice (Figure 6D). In contrast, depletion of FRA1 in two luminal-like, hormone receptor-positive (ER[+]/PR[+]) breast cancer cell lines, MCF7-Ras and T47D, did not affect their proliferation, expression of EMT-associated markers, tumor formation, or tumor growth (Figures S5A–S5C). These observations suggested that FRA1 was important for the tumorigenic potential of breast cancer cells forming basal-like or triple-negative tumors but not those forming luminal tumors.

This led us to speculate that FRA1 expression might be restricted to the more mesenchymal, CSC-enriched compartments within basal-like human breast tumors. Previous studies have shown that purified CD44^{+} or protein C receptor-positive (PROCR^{+}) cells tend to be enriched for CSCs in primary human tumors, whereas the CD24^{+} fraction was depleted of these cells (Al-Hajj et al., 2003; Shipitsin et al., 2007). Both CD44^{+}- and PROCR^{+}-purified cells also demonstrated elevated mRNA expression of *VIM* (403x), *FN1* (48x) and *TWIST* (6.6x) (Shipitsin et al., 2007). Thus, we further analyzed the expression of *FOSL1* and *FOS* in these CD44^{+}/PROCR^{+} or CD24^{+} cells isolated from human tumors (Shipitsin et al., 2007). Across multiple specimens, *FOSL1* was upregulated in the CD44^{+}/PROCR^{+} fraction, while *FOS* was elevated in the CD24^{+} fraction (Figure S5D) providing additional support that *FOSL1* expression is associated with CSC-enriched CD44^{+} populations bearing mesenchymal properties.

Effects of the Twist and Snail EMT-TFs on FRA1 expression

The increased expression of FRA1 in the EMT TF-induced mesenchymal cells and NAMECs correlated closely with the abundance of several EMT-TFs, suggesting that the latter might directly induce *FOSL1* mRNA expression. To test this notion, we fused ER to either Twist or Snail (HMLE-Twist-ER and HMLE-Snail-ER) (Mani et al., 2008) and demonstrated that activation of Twist or Snail upon tamoxifen exposure led to increased levels of *FOSL1* mRNA in a time-dependent manner (Figure 6E). We next assessed whether Twist or Snail bound at the *FOSL1* promoter using chromatin immunoprecipitation (ChIP) and could detect their binding at the transcription start site and within the first intron of *FOSL1* (Figure 6F). These regions contained E-box motifs (CANNTG), which Twist and Snail are known to bind. In contrast, the promoter of *FOS* was only weakly enriched for Twist and Snail binding (Figure 6F). Together, these data suggested that *FOSL1* was a direct target of Twist and of Snail.

To determine whether the ability of FRA1 to drive gene transcription was dependent on the expression of EMT-TFs, we utilized a luciferase reporter containing the sequence of a previously reported FRA1-bound gene promoter (FRA1-wild-type-binding site: FRA1-WT-BS) as well as a mutant FRA1-binding construct (FRA1-mut-BS) (Stinson et al., 2011). In NAMECs, knockdown of FRA1 abrogated luciferase activity of the FRA1-WT-BS but not FRA1-mut-BS (Figure 6G, left panel). Similarly, knockdown of TWIST or SNAIL diminished FRA1-dependent expression of the FRA1-WT-BS reporter (Figure 6G, left panel). *FOSL1* mRNA expression was also reduced upon either TWIST or SNAIL knockdown (Figure 6H).

In a reverse experiment, we overexpressed FRA1 in the NAMEC11 cell line, which had undergone a partial EMT. Overexpression of FRA1 induced FRA1-WT-BS but not FRA1-

mut-BS luciferase activity (Figure 6G, right panel). Likewise, Twist and Snail overexpression in these cells was able to induce transcription of the FRA1-WT-BS reporter (Figure 6G, right panel). The wild-type AP-1 reporter containing tandem repeats of AP-1 response element was used as a positive control (Figure 6G). Therefore, these various lines of evidence confirmed that *FOSL1* levels were transcriptionally regulated by two master EMT-TFs and in a direct manner.

To demonstrate that FRA1 plays a functionally significant role downstream of EMT-TFs, we activated Twist or Snail in HMLE-Twist-ER or HMLE-Snail-ER cells in the presence or absence of two different FRA1 shRNAs, and assessed the ability of these cells to transit into the mesenchymal state. HMLE-Twist-ER and HMLE-Snail-ER cells that expressed control shRNA underwent an EMT within one week after 4-OH-tamoxifen exposure (Figures 7A and 7B). However, FRA1-depleted cells were blocked in their ability to undergo an EMT upon Twist or Snail activation, and retained their epithelial phenotype (Figures 7A and 7B). These observations reinforced our conclusion that FRA1 acts as an effector of the EMT program that is required for its execution.

Relevance of FRA1 and PKCα expression to clinical breast cancer

The functional significance of FRA1 in mediating cell-state transition and in maintaining CSCs led us to wonder whether its expression might also be relevant to clinical breast cancer. We speculated that *FOSL1* expression was restricted to basal B and triple-negative breast cancer (TNBC) tumors and cell lines, as these bear strong molecular hallmarks of cells that have activated an EMT program (Shipitsin et al., 2007). These subtypes are also thought to contain a high representation of CSCs, thereby favoring relapse, metastasis and poor overall survival. Indeed, *FOSL1* mRNA levels, but not those of other AP-1 subunits, were elevated in the basal B subtype of breast cancer cell lines surveyed, whereas its levels were reduced in the basal A cell lines and were essentially undetectable in all luminal subtype cell lines (Neve et al., 2006) (Figure S6A).

From a compendium of clinical datasets, we observed high *FOSL1* expression significantly correlated with poor distant metastasis-free survival (DMFS), while high *FOS* or *FOSB* expression associated with better survival (Figures 7C and S6B). The expression levels of other AP-1 subunits did not predict patient outcome (Figure S6B). Additionally, higher *PKCα* and *FOSL1* mRNA expression was significantly associated with HER2−, ER− or PR− status, as well as with triple-negative tumors (Figure 7D). Their expression was also elevated in tumors bearing *BRCA1* mutations and in breast cancer cell lines containing *p53* mutations (Figure 7D). Moreover, *FOSL1*, *PDGFRA* and *PDGFRB* mRNAs were more highly expressed in the claudin-low subtype of breast cancer that is thought to express the most mesenchymal properties (Figure S6C).

To exclude the possibility that *FOSL1* mRNA expression was derived from infiltrating stromal cells, we examined its protein expression in breast tumor microarrays derived from patients whose tumors had been scored for tumor grade. Moderate-to-strong nuclear FRA1 staining was present predominantly in the neoplastic cells of Grade 3 tumors that were typically hormone receptors-negative but far less commonly in Grade 1 and Grade 2 tumors, or in the normal mammary epithelium (Figure 7E). A similar trend could be observed with

cytoplasmic and membrane-localized PKCα in which moderate-strong staining was most common in Grade 3 tumors relative to Grade 1 and 2 tumors (Figure 7E). Taken together, these results reinforced the notion that FRA1, along with PKCα, function as important mediators of the behavior of aggressive basal-like and TNBCs.

In light of the findings that PKCα inhibitors, administered systemically, could inhibit the growth of breast cancer cells bearing mesenchymal traits and the observation that triple-negative breast tumors tend to express elevated levels of PKCα, we tested whether PKCα inhibition could be useful therapeutically against patient-derived tumor samples. We generated three patient-derived breast cancer xenografts from triple-negative tumors (EL12-58, EL12-15 and EL11-26) that had been serially passaged in NOD-SCID mice following their removal from patients. We then transplanted these tumor fragments orthotopically into a fresh set of female NOD-SCID mice and on the same day, subjected them to either a PKCα inhibitor or vehicle control that was administered intraperitoneally daily for six weeks. With all three xenograft lines, tumors that formed in the PKCα inhibitor-treated mice were consistently smaller (EL12-15: 65.7%, EL11-26: 53.3%, EL12-58: 39.5%) than the control group (Figure 7F). Thus, inhibition of PKCα appeared to be a potentially useful strategy for targeting triple-negative breast tumors.

DISCUSSION

We and others have argued previously that effective treatment of carcinomas depends upon the elimination of minority CSCs in addition to the majority non-CSC cells in these tumors (Creighton et al., 2009; Dalerba et al., 2007; Gupta et al., 2009). This led us to exploit the observation that the EMT program generates cells that are enriched for stem cell and CSC properties in order to identify signaling networks that are preferentially utilized in the cellular products of an EMT (Figure 8). Our present findings demonstrate that PKCα is a central regulatory node activated by PDGFR in CSC-enriched populations. While PKCα has been implicated in promoting cancer progression (Griner and Kazanietz, 2007; Lonne et al., 2010), its connection to cell-state transitions and CSCs has been unclear. As a proof-of-principle, we showed the pharmacologic inhibition of PKCα can target breast CSCs selectively and that clinically effective compounds inhibiting PKCα may prove therapeutically useful for treating certain breast tumors.

The selective dependence of the epithelial versus mesenchymal MECs on the function of EGFR and PDGFR is clinically relevant, because EGFR inhibitors are being tested in clinical trials or in clinical use but often resulting in limited clinical responses (Carey et al., 2010). Several studies have pointed out that such inhibitors enrich for CSCs and can lead to the outgrowth of more aggressive, chemotherapy-resistant tumor cell populations (Buck et al., 2007; Thomson et al., 2005). These studies suggest that the presence of epithelial- and mesenchymal-like carcinoma cells within tumors requires the elimination of both cell types.

The EMT program is initially required for invasion and dissemination of tumor cells whereas MET has been demonstrated to promote colonization and metastatic outgrowth (Ocana et al., 2012; Tsai et al., 2012). An increasing number of observations suggest that both tumor-initiation and metastatic outgrowth depend on coexisting subpopulations of

epithelial and mesenchymal subpopulations; conversely tumors containing exclusively one or the other subpopulation appear to be poorly suited in enabling both of these processes (Brabletz, 2012; Celia-Terrassa et al., 2012; Ocana et al., 2012). This implies that while the inhibition of cancer cells bearing a mesenchymal phenotype could be useful for preventing tumor-initiation and/or dissemination, such a therapeutic strategy needs to be complemented with treatments that target already-established metastases and their complements of non-CSC epithelial cells. Moreover, the EMT should be viewed as generating a spectrum of phenotypic states depending on the extent to which this program is completed by epithelial cells, and partial completion of this program may be essential for the formation of CSCs and thus the founding of metastases. Future work will require more detailed measurements of the extent to which the various intermediate states depend on the epithelial versus mesenchymal signaling circuits described here.

Our initial efforts to distinguish molecular features between mammary CSCs and non-CSCs have led to the identification of kinase inhibitors that may be useful in preclinical models of human breast cancer. We speculate that the EMT program may also be adopted by other carcinoma cell types to drive tumor progression and metastasis. If so, the approach used to identify therapeutic compounds and pathways unique to mammary carcinoma CSCs described here may be extended to target CSCs present in the tumors arising from other epithelial tissues.

EXPERIMENTAL PROCEDURES

Kinase inhibitor screen

Kinase inhibitors and other biochemicals were obtained from sources listed in the Supplemental Information. To set up the screen, 75,000 NAMEC-Tom and 15,000 HMLE-GFP cells were seeded into each well of a 6-well tissue culture plate. The following day, fresh media containing inhibitors were added. For control treatment, DMSO was added. Fresh media containing inhibitors were replaced daily during the six day period. For analysis, cells were trypsinized and flow cytometry was performed to analyze the proportion of surviving cells relative to DMSO-treated control for NAMEC-Tom or HMLE-GFP cells. To test the effects of these inhibitors on CSCs and non-CSCs, NAMEC-RAS-Tom and HMLE-RAS-GFP were used in similar co-mixed experiments.

Cell Lines and Cell Culture

HMLE cells and NAMECs were maintained in MEGM (Lonza). Other commonly used breast cancer cell lines are listed in Supplemental Information. HMLE were generated from HMECs immortalized using retroviral vectors to express the catalytic subunit of the human telomerase enzyme, hTERT and the SV-40 Large T antigen. NAMECs were isolated based on the observation that mesenchymal cells were less adherent than epithelial cells to tissue culture surfaces. HMLE cells were grown to 50% confluency, followed by differential trypsinization for one minute with 0.05% trypsin. Detached cells were collected and re-plated at approximately 200 cells per well of a 24-well plate. Upon expansion, wells were screened for populations with a mesenchymal phenotype that could be stably propagated.

Gene expression microarray and analyses

Total RNA was extracted and expression profiling of coding genes was carried out using Illumina HumanRef-8 v2 BeadArrays. Gene expression data from Illumina array is normalized by quantile normalization. Differential genes are called using LIMMA with $p<0.05$ and fold change > 1.2.

Patient-derived breast cancer xenograft establishment and therapy

Primary human breast cancer samples were obtained from the Dana-Farber Cancer Institute with patients' consent and institutional review board approval. These samples were subsequently de-identified to protect patient confidentiality. Patient-derived breast tumor fragments (approximately $3\times1\times1$ mm) were inserted bilaterally into the inguinal mammary fat pads of 6–8 week-old NOD-SCID-IL2Rγc$^{-/-}$ female mice for initial establishment of tumors within 2 hr of surgery, and subsequently expanded in NOD-SCID mice once established. Established TNBC tumors (EL12-15, EL12-58 and EL11-26) were implanted into cohorts of 6–8 week-old female NOD-SCID mice. Treatment was initiated at the time of tumor implantation and the mice were randomized into two groups: vehicle (10% DMSO in saline) and treatment (Ro-31-8220, 5 mg/kg/day intraperitoneally). Tumors were collected and weighed after six, eight or 11 weeks. All research involving animals complied with protocols approved by the MIT Committee on Animal Care.

Supplementary Material

Refer to Web version on PubMed Central for supplementary material.

Acknowledgments

References

Abate C, Marshak DR, Curran T. Fos is phosphorylated by p34cdc2, cAMP-dependent protein kinase and protein kinase C at multiple sites clustered within regulatory regions. Oncogene. 1991; 6:2179–2185. [PubMed: 1766667]

Ailles LE, Weissman IL. Cancer stem cells in solid tumors. Curr Opin Biotechnol. 2007; 18:460–466. [PubMed: 18023337]

Al-Hajj M, Wicha MS, Benito-Hernandez A, Morrison SJ, Clarke MF. Prospective identification of tumorigenic breast cancer cells. Proc Natl Acad Sci U S A. 2003; 100:3983–3988. [PubMed: 12629218]

Blick T, Widodo E, Hugo H, Waltham M, Lenburg ME, Neve RM, Thompson EW. Epithelial mesenchymal transition traits in human breast cancer cell lines. Clin Exp Metastasis. 2008; 25:629–642. [PubMed: 18461285]

Brabletz T. To differentiate or not--routes towards metastasis. Nat Rev Cancer. 2012; 12:425–436. [PubMed: 22576165]

Buck E, Eyzaguirre A, Barr S, Thompson S, Sennello R, Young D, Iwata KK, Gibson NW, Cagnoni P, Haley JD. Loss of homotypic cell adhesion by epithelial-mesenchymal transition or mutation limits

sensitivity to epidermal growth factor receptor inhibition. Mol Cancer Ther. 2007; 6:532–541. [PubMed: 17308052]

Cameron AJ, Escribano C, Saurin AT, Kostelecky B, Parker PJ. PKC maturation is promoted by nucleotide pocket occupation independently of intrinsic kinase activity. Nat Struct Mol Biol. 2009; 16:624–630. [PubMed: 19465915]

Carey L, Winer E, Viale G, Cameron D, Gianni L. Triple-negative breast cancer: disease entity or title of convenience? Nat Rev Clin Oncol. 2010; 7:683–692. [PubMed: 20877296]

Celia-Terrassa T, Meca-Cortes O, Mateo F, de Paz AM, Rubio N, Arnal-Estape A, Ell BJ, Bermudo R, Diaz A, Guerra-Rebollo M, et al. Epithelial-mesenchymal transition can suppress major attributes of human epithelial tumor-initiating cells. J Clin Invest. 2012; 122:1849–1868. [PubMed: 22505459]

Creighton CJ, Li X, Landis M, Dixon JM, Neumeister VM, Sjolund A, Rimm DL, Wong H, Rodriguez A, Herschkowitz JI, et al. Residual breast cancers after conventional therapy display mesenchymal as well as tumor-initiating features. Proc Natl Acad Sci U S A. 2009; 106:13820–13825. [PubMed: 19666588]

Dalerba P, Cho RW, Clarke MF. Cancer stem cells: models and concepts. Annu Rev Med. 2007; 58:267–284. [PubMed: 17002552]

Eferl R, Wagner EF. AP-1: a double-edged sword in tumorigenesis. Nat Rev Cancer. 2003; 3:859–868. [PubMed: 14668816]

Ginestier C, Hur MH, Charafe-Jauffret E, Monville F, Dutcher J, Brown M, Jacquemier J, Viens P, Kleer CG, Liu S, et al. ALDH1 is a marker of normal and malignant human mammary stem cells and a predictor of poor clinical outcome. Cell Stem Cell. 2007; 1:555–567. [PubMed: 18371393]

Gould CM, Antal CE, Reyes G, Kunkel MT, Adams RA, Ziyar A, Riveros T, Newton AC. Active site inhibitors protect protein kinase C from dephosphorylation and stabilize its mature form. J Biol Chem. 2011; 286:28922–28930. [PubMed: 21715334]

Griner EM, Kazanietz MG. Protein kinase C and other diacylglycerol effectors in cancer. Nat Rev Cancer. 2007; 7:281–294. [PubMed: 17384583]

Gruda MC, Kovary K, Metz R, Bravo R. Regulation of Fra-1 and Fra-2 phosphorylation differs during the cell cycle of fibroblasts and phosphorylation in vitro by MAP kinase affects DNA binding activity. Oncogene. 1994; 9:2537–2547. [PubMed: 8058317]

Gupta PB, Onder TT, Jiang G, Tao K, Kuperwasser C, Weinberg RA, Lander ES. Identification of selective inhibitors of cancer stem cells by high-throughput screening. Cell. 2009; 138:645–659. [PubMed: 19682730]

Kakumoto K, Sasai K, Sukezane T, Oneyama C, Ishimaru S, Shibutani K, Mizushima H, Mekada E, Hanafusa H, Akagi T. FRA1 is a determinant for the difference in RAS-induced transformation between human and rat fibroblasts. Proc Natl Acad Sci U S A. 2006; 103:5490–5495. [PubMed: 16569692]

Kang JH, Toita R, Kim CW, Katayama Y. Protein kinase C (PKC) isozyme-specific substrates and their design. Biotechnol Adv. 2012

Kolch W, Heidecker G, Kochs G, Hummel R, Vahidi H, Mischak H, Finkenzeller G, Marme D, Rapp UR. Protein kinase C alpha activates RAF-1 by direct phosphorylation. Nature. 1993; 364:249–252. [PubMed: 8321321]

Lonne GK, Cornmark L, Zahirovic IO, Landberg G, Jirstrom K, Larsson C. PKCalpha expression is a marker for breast cancer aggressiveness. Mol Cancer. 2010; 9:76. [PubMed: 20398285]

Mani SA, Guo W, Liao MJ, Eaton EN, Ayyanan A, Zhou AY, Brooks M, Reinhard F, Zhang CC, Shipitsin M, et al. The epithelial-mesenchymal transition generates cells with properties of stem cells. Cell. 2008; 133:704–715. [PubMed: 18485877]

Morel AP, Lievre M, Thomas C, Hinkal G, Ansieau S, Puisieux A. Generation of breast cancer stem cells through epithelial-mesenchymal transition. PLoS One. 2008; 3:e2888. [PubMed: 18682804]

Neve RM, Chin K, Fridlyand J, Yeh J, Baehner FL, Fevr T, Clark L, Bayani N, Coppe JP, Tong F, et al. A collection of breast cancer cell lines for the study of functionally distinct cancer subtypes. Cancer Cell. 2006; 10:515–527. [PubMed: 17157791]

Newton AC. Protein kinase C: structural and spatial regulation by phosphorylation, cofactors, and macromolecular interactions. Chem Rev. 2001; 101:2353–2364. [PubMed: 11749377]

Nieto MA. The ins and outs of the epithelial to mesenchymal transition in health and disease. Annu Rev Cell Dev Biol. 2011; 27:347–376. [PubMed: 21740232]

Ocana OH, Corcoles R, Fabra A, Moreno-Bueno G, Acloque H, Vega S, Barrallo-Gimeno A, Cano A, Nieto MA. Metastatic colonization requires the repression of the epithelial-mesenchymal transition inducer Prrx1. Cancer Cell. 2012; 22:709–724. [PubMed: 23201163]

Pece S, Tosoni D, Confalonieri S, Mazzarol G, Vecchi M, Ronzoni S, Bernard L, Viale G, Pelicci PG, Di Fiore PP. Biological and molecular heterogeneity of breast cancers correlates with their cancer stem cell content. Cell. 2010; 140:62–73. [PubMed: 20074520]

Rhee SG. Regulation of phosphoinositide-specific phospholipase C. Annu Rev Biochem. 2001; 70:281–312. [PubMed: 11395409]

Saito Y, Hojo Y, Tanimoto T, Abe J, Berk BC. Protein kinase C-alpha and protein kinase C-epsilon are required for Grb2-associated binder-1 tyrosine phosphorylation in response to platelet-derived growth factor. J Biol Chem. 2002; 277:23216–23222. [PubMed: 11940581]

Sarrio D, Rodriguez-Pinilla SM, Hardisson D, Cano A, Moreno-Bueno G, Palacios J. Epithelial-mesenchymal transition in breast cancer relates to the basal-like phenotype. Cancer Res. 2008; 68:989–997. [PubMed: 18281472]

Scheel C, Eaton EN, Li SH, Chaffer CL, Reinhardt F, Kah KJ, Bell G, Guo W, Rubin J, Richardson AL, Weinberg RA. Paracrine and autocrine signals induce and maintain mesenchymal and stem cell states in the breast. Cell. 2011; 145:926–940. [PubMed: 21663795]

Shipitsin M, Campbell LL, Argani P, Weremowicz S, Bloushtain-Qimron N, Yao J, Nikolskaya T, Serebryiskaya T, Beroukhim R, Hu M, et al. Molecular definition of breast tumor heterogeneity. Cancer Cell. 2007; 11:259–273. [PubMed: 17349583]

Stinson S, Lackner MR, Adai AT, Yu N, Kim HJ, O'Brien C, Spoerke J, Jhunjhunwala S, Boyd Z, Januario T, et al. TRPS1 targeting by miR-221/222 promotes the epithelial-to-mesenchymal transition in breast cancer. Sci Signal. 2011; 4:ra41. [PubMed: 21673316]

Thiery JP, Acloque H, Huang RY, Nieto MA. Epithelial-mesenchymal transitions in development and disease. Cell. 2009; 139:871–890. [PubMed: 19945376]

Thomson S, Buck E, Petti F, Griffin G, Brown E, Ramnarine N, Iwata KK, Gibson N, Haley JD. Epithelial to mesenchymal transition is a determinant of sensitivity of non-small-cell lung carcinoma cell lines and xenografts to epidermal growth factor receptor inhibition. Cancer Res. 2005; 65:9455–9462. [PubMed: 16230409]

Tsai JH, Donaher JL, Murphy DA, Chau S, Yang J. Spatiotemporal regulation of epithelial-mesenchymal transition is essential for squamous cell carcinoma metastasis. Cancer Cell. 2012; 22:725–736. [PubMed: 23201165]

Waddell N, Cocciardi S, Johnson J, Healey S, Marsh A, Riley J, da Silva L, Vargas AC, Reid L, Simpson PT, et al. Gene expression profiling of formalin-fixed, paraffin-embedded familial breast tumours using the whole genome-DASL assay. J Pathol. 2010; 221:452–461. [PubMed: 20593485]

SIGNIFICANCE

Conventional cancer therapeutics tend to preferentially eliminate the non-CSCs within a tumor, leaving behind residues of more resistant CSCs that can subsequently generate clinical relapses, indicating the need to specifically target the CSCs within tumors. The identification of key regulatory mechanisms that distinguish CSCs from non-CSCs is therefore critical for CSC-targeted therapy. We find that the PKCα signaling network is activated specifically in CSCs, rendering them preferentially susceptible to specific pharmacologic agents. In addition, we uncovered FRA1 to be a key transcription factor downstream of PKCα that drives CSC function. The inhibition of either PKCα or FRA1 can abolish tumor initiation, highlighting the potential therapeutic value of targeting these proteins in epithelial cancers such as breast cancer.

HIGHLIGHTS

- Inhibition of PKCα preferentially targets breast cancer stem cells

- Activation of an EMT program induces a shift from EGFR to PDGFR signaling

- Activation of an AP-1 molecular switch involving c-FOS and FRA1 in CSCs

- FRA1 is required for the EMT phenotype and tumor-initiation ability
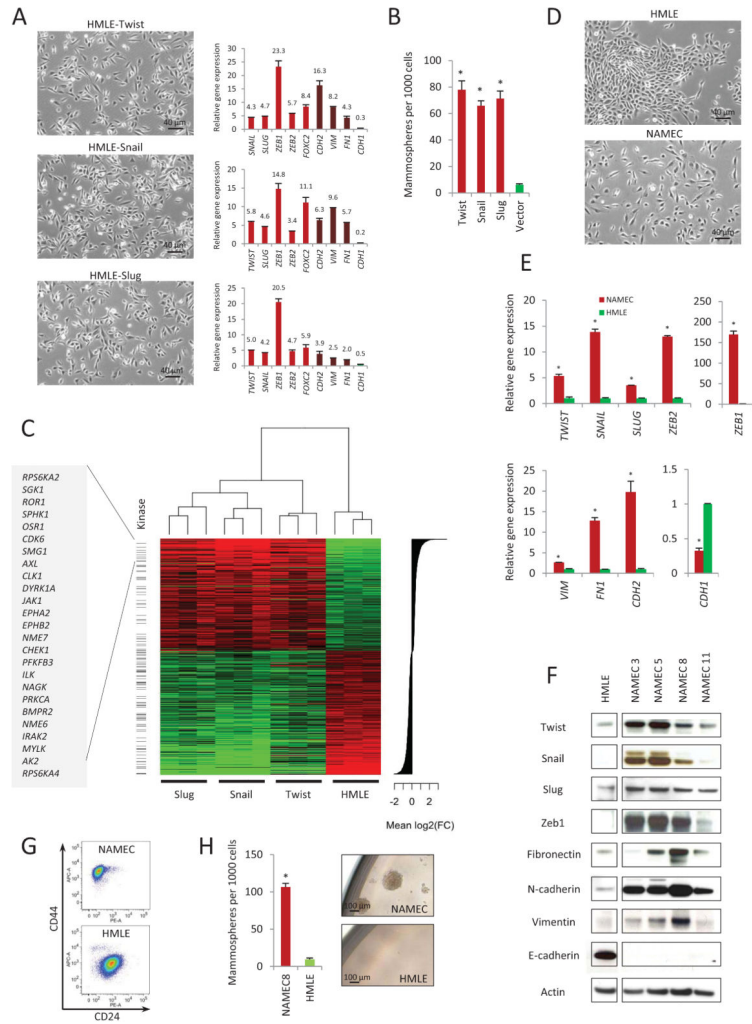
Figure 1. Global gene expression analyses reveal differentially regulated kinases whose mRNA expression are altered following EMT

(A) Representative phase contrast images of the indicated cell lines (left) and quantitative PCR for gene expression of EMT markers in these cell lines relative to HMLE-vector cells (right). Numbers denote fold change. Scale bar: 40 μm.

(B) Mammosphere-forming ability of HMLE cells transduced with Twist, Snail or Slug.

(C) Heat map of the top differentially regulated genes between HMLE-Twist, HMLE-Snail, HMLE-Slug and control cells (fold change > 1.2).

(D) Phase contrast images of NAMEC and HMLE cells. Scale bar: 40 μm.

(E) Quantitative PCR for gene expression of EMT markers in NAMEC8 and HMLE cells.

(F) Western blots of EMT-associated proteins in NAMECs and HMLE cells. Samples were loaded and analyzed on the same blot.

(G) Flow cytometry analysis for the expression of CD44 and CD24 surface antigens on NAMECs and HMLE cells.

(H) Mammosphere-forming ability of NAMECs and HMLE cells.

*$p < 0.05$. Data presented as mean ± s.e.m. See also Table S1 and Figure S1.
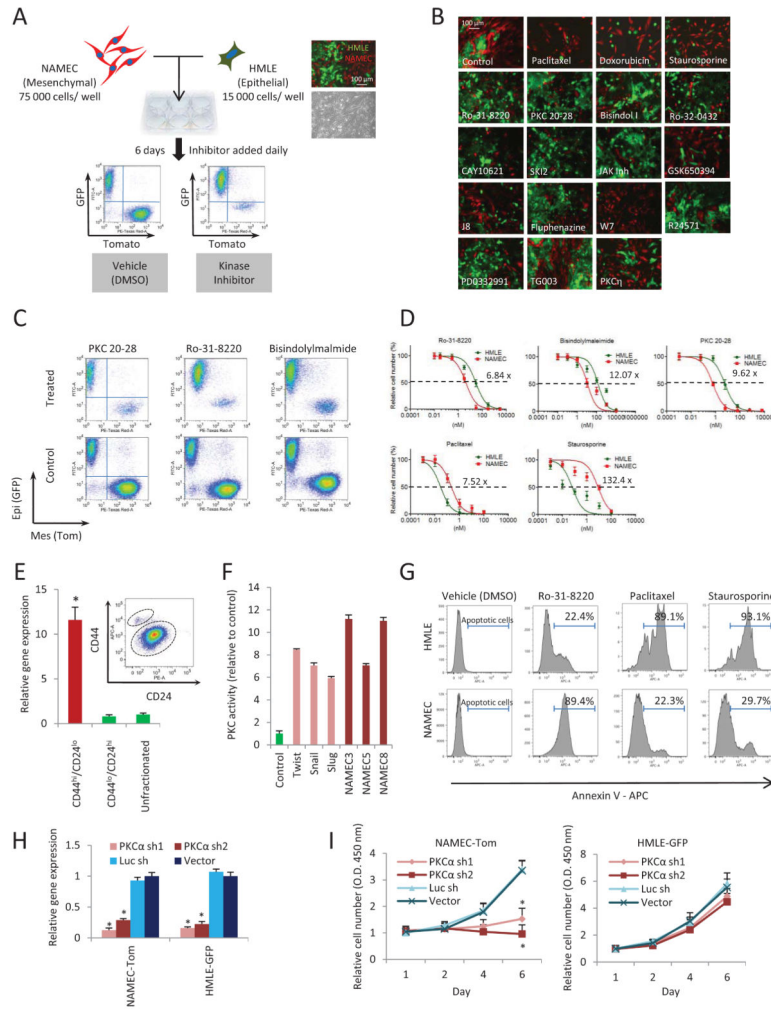
Figure 2. PKCα inhibition selectively targets cells that have undergone an EMT and are enriched for stem cell properties

(A) Approach for testing kinase inhibitors to identify stem cell-specific compounds. NAMEC-Tom and HMLE-GFP cells were co-mixed and seeded for 24 hr prior to daily inhibitor treatment. Viable cells were analyzed after six days by flow cytometry to determine the proportion of NAMEC-Tom or HMLE-GFP cells.

(B) The proportion of surviving NAMEC-Tom and HMLE-GFP cells as visualized by fluorescence microscopy after six days of inhibitor treatment.

(C) Viable cell populations were analyzed by flow cytometry that segregated and counted NAMEC-Tom and HMLE-GFP cells after treatment with PKCα inhibitors. Cell numbers of each population were normalized to corresponding NAMEC-Tom or HMLE-GFP cells of DMSO-treated controls.

(D) Dose-response curves of NAMEC-Tom and HMLE-GFP cells treated with PKCα inhibitors, paclitaxel or staurosporine. The difference in LC_{50} between NAMEC-Tom and HMLE-GFP cells at each inhibitor is indicated. Curves for each cell type were generated using non-linear regression curve fit with the variable slope model.

(E) Quantitative PCR for *PKCα* mRNA level in CD44^{hi}/CD24^{lo}, CD44^{lo}/CD24^{hi} and unfractionated cell compartments of HMLE cells.

(F) Levels of total PKC kinase activity in EMT-TF-induced HMLE and NAMEC cells relative to HMLE control cells.

(G) Measurement of apoptosis by Annexin V-APC in mixed NAMEC-Tom and HMLE-GFP cells treated with Ro-31-8220 for three days.

(H) Quantitative PCR for validation of PKCα RNAi knockdown in NAMEC-Tom and HMLE-GFP cells three days after puromycin selection. * denotes significantly different from Luc sh control.

(I) Effects of PKCα RNAi on the growth kinetics of NAMEC-Tom and HMLE-GFP cells as measured by WST assay. * denotes significantly different from Luc sh control.

*$p<0.05$. Data presented as mean ± s.e.m. See also Figure S2.
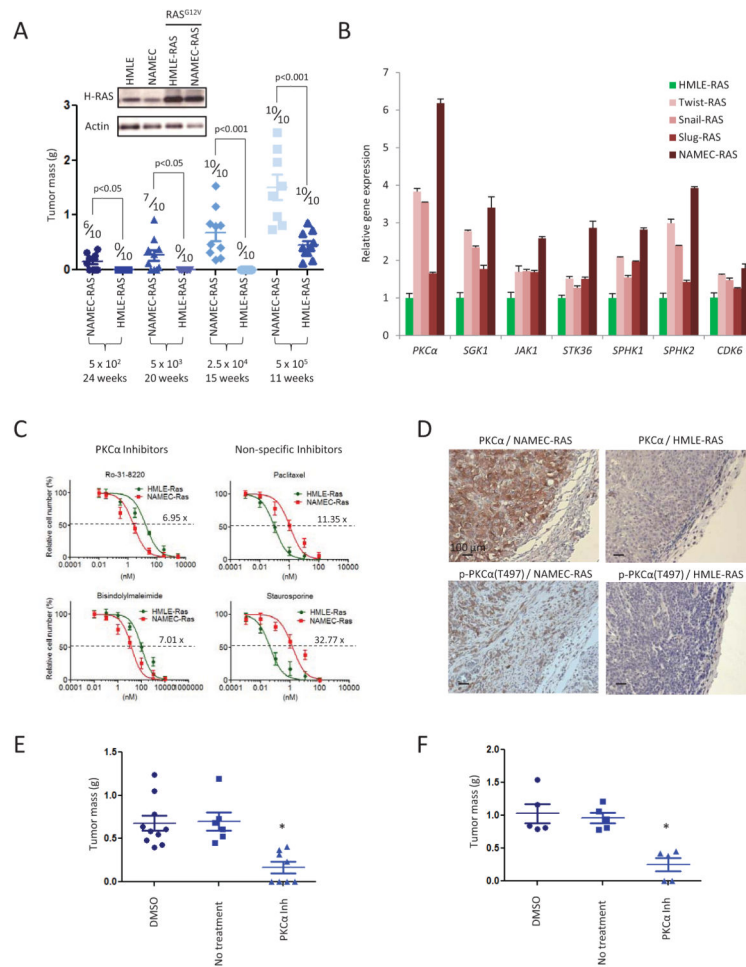
Figure 3. Cell state-specific kinase expression is conserved upon oncogenic RAS^{G12V} transformation and in CSCs

(A) Assessment of the tumorigenicity of NAMEC-RAS or HMLE-RAS cells injected subcutaneously into NOD-SCID mice at limiting dilutions of cells, as determined by tumor mass. Numbers indicate the frequency of tumor formation. Western blot indicates levels of RAS expression.

(B) Quantitative PCR for gene expression of selected kinases in HMLE-Twist-RAS, HMLE-Snail-RAS, HMLE-Slug-RAS and NAMEC-RAS cells relative to HMLE-RAS cells.

(C) Dose-response curves of NAMEC-Tom-RAS and HMLE-GFP-RAS cells treated with PKCα inhibitors, paclitaxel or staurosporine. Differential sensitivity to treatment at LC$_{50}$ is indicated.

(D) Immuno-histochemistry detection of total PKCα and p-PKCα^{T497} in sections of equivalent size (~0.3 g) NAMEC-RAS and HMLE-RAS tumors. NAMEC-RAS tumors were 15 weeks after inoculation of 2.5×10^4 cells and HMLE-RAS tumors were 11 weeks after inoculation of 5×10^5 cells.

(E) Assessment of the tumorigenicity of subcutaneously xenografted NAMEC-RAS cells (5×10^4) in mice treated with daily intraperitoneal administration of the indicated agents, as determined by tumor mass. Treatments began on the same day as the cells were implanted. Tumors were collected 15 weeks post-implantation.

(F) Assessment of the tumorigenicity of established NAMEC-RAS tumors following treatment with the indicated agents. NAMEC-RAS cells (5×10^4) were subcutaneously xenografted in mice and allowed to reach approximately 2 mm in diameter after four weeks. Subsequently, mice were treated with daily intraperitoneal administration of the indicated agents for 30 days. Tumors were collected six weeks later and tumor masses were determined.

*p<0.005. Data presented as mean ± s.e.m.
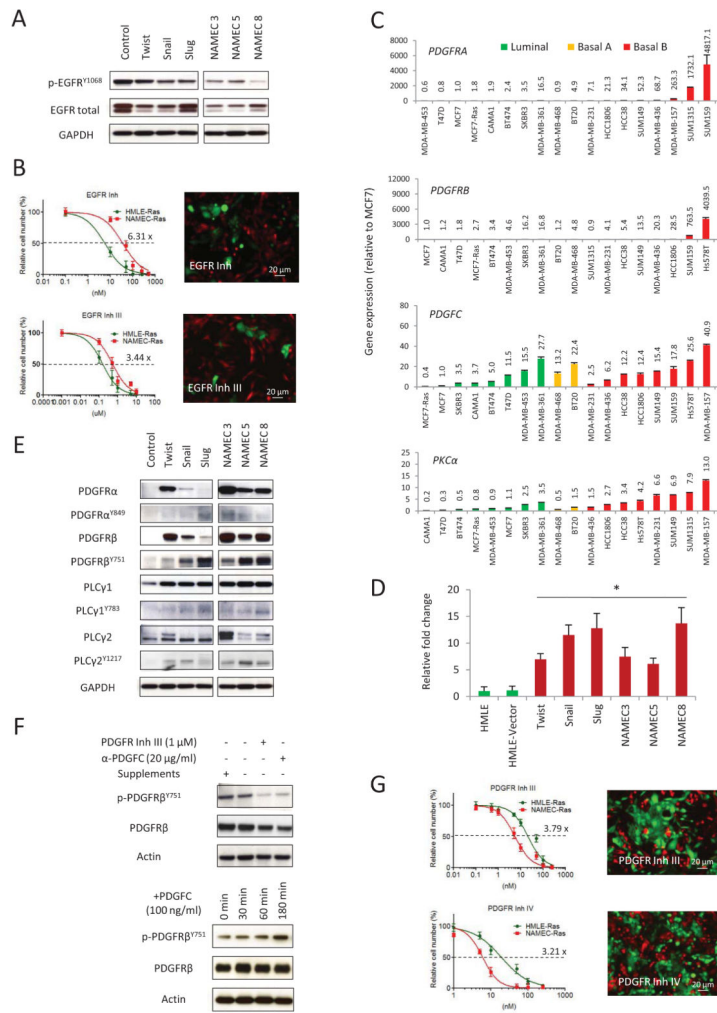
Figure 4. EMT induces a switch from EGFR to PDGFR signaling

(A) Western blots of total and p-EGFR^{Y1068} in the indicated EMT-TF-induced HMLE and NAMEC cells. Samples were loaded and analyzed on the same blot.

(B) Dose response curves (left) of the sensitivities of HMLE-RAS-GFP and NAMEC-RAS-Tom cells to EGFR inhibitors. The difference in fold sensitivity between both cell types at LC$_{50}$ is indicated. Representative immunofluorescent images are shown at the right.

(C) Quantitative PCR for *PDGFRA*, *PDGFRB*, *PDGFC* and *PKCα* mRNA expression in breast cancer cell lines. Numbers indicate fold change.

(D) Quantitative PCR for *PDGFC* expression in mesenchymal and epithelial cells. * denotes significantly different from HMLE or HMLE-vector, p<0.05.

(E) Western blots of PDGFRα, PDGFRβ, PLCγ1 and PLCγ2, along with protein phosphorylation, in NAMECs and EMT-TF-induced cells. Sample loading controls (GAPDH) were the same as Figure 4A. Samples were loaded and analyzed on the same blot.

(F) Western blot analysis of NAMECs cultured in the absence of growth supplements (bovine pituitary extract, EGF, hydrocortisone and insulin) and treated with either a PDGFC neutralizing antibody (20 μg/ml) or a PDGFR inhibitor (1 μM) (top), or upon exposure to PDGFC (100 ng/ml) (bottom). PDGFR activity is represented by the phosphorylation of PDGFRβ^{Y751}.

(G) Dose response curves (left) of HMLE-RAS-GFP and NAMEC-RAS-Tom cells to PDGFR inhibitors. The difference in fold sensitivity between both cell types at LC_{50} is indicated. Representative immunofluorescent images are shown at the right. Data presented as mean ± s.e.m. See also Figure S3.
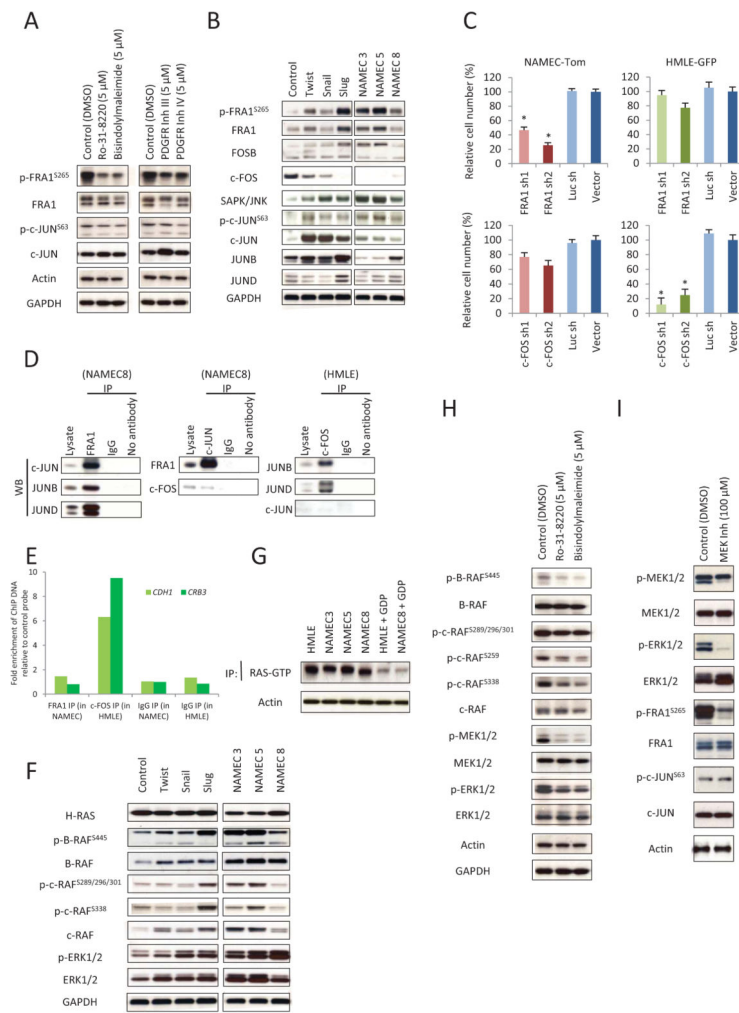
Figure 5. PDGFR signaling results in PKCα and ERK1/2 activation that induces FRA1

(A) Western blot analysis of the effects of inhibiting PKCα (using Ro-31-8220 or bisindolylmalmide I) or PDGFRα/β (using PDGFR Inh III or PDGFR Inh IV) for 30 minutes on the phosphorylation status of FRA1 and c-JUN in NAMECs.

(B) Western blots of AP-1 family member subunits in epithelial and mesenchymal cell lines. Samples were loaded and analyzed on the same blot.

(C) Relative cell number analyses of the effects of FRA1 or c-FOS knockdown on the viability of NAMEC-Tom and HMLE-GFP cells. * denotes significantly different from vector control, p<0.05. Data presented as mean ± s.e.m.

(D) Western blots for proteins immunoprecipitated with FRA1 or c-JUN antibodies in NAMECs, and with c-FOS antibody in HMLE cells. Whole cell lysates were used as positive controls while pull-down with IgG or without an antibody was performed as negative controls.

(E) Occupancy of c-FOS and FRA1 on the promoters of *CDH1* and *CRB3* (encoding Crumb3). A normalization probe for non-enriched region is located within intron 1 (*CDH1*) or intron 3 (*CRB3*). Control ChIP was performed with an IgG antibody.

(F) Western blots of total and phosphorylated B-RAF, c-RAF and ERK1/2 in TF-induced EMT and NAMEC cells. Sample loading controls (GAPDH) were the same as Figure 5B. Samples were loaded and analyzed on the same blot.

(G) The amount of GTP-bound Ras was compared between epithelial and mesenchymal cell states by immunoprecipitation with Raf-Ras Binding Domain (RBD) beads followed by blotting with a pan-Ras antibody. As a negative control, lysates were treated

with GDP which blocked the ability of Ras to bind Raf-RBD beads. β-actin from whole cell lysate (prior to IP) was used as a loading control.

(H) Western blots of phosphorylated proteins of B-RAF, c-RAF, MEK1/2 and ERK1/2 in NAMEC cells following treatment with PKCα inhibitors for 30 minutes.

(I) Western blots of p-FRA1 levels in NAMEC cells following MEK inhibition for 30 minutes.

See also Figure S4.
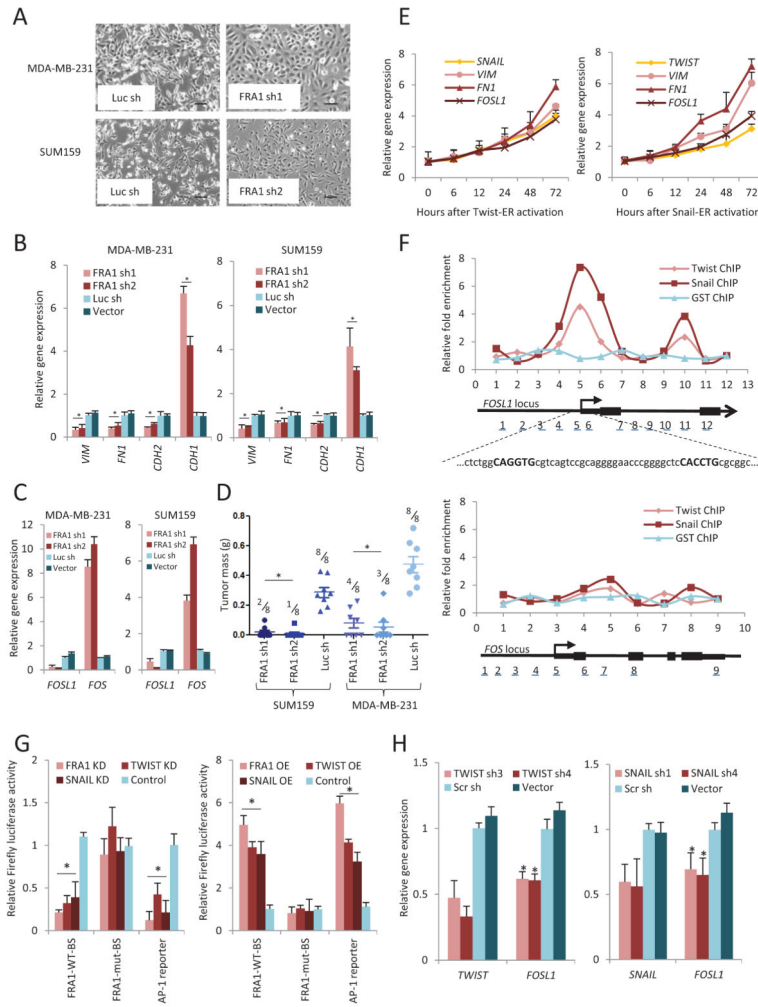
Figure 6. FRA1 is a transcriptional target of Twist and Snail that is indispensible for tumorigenicity of basal-like breast cancer cells

(A) Phase contrast images showing the morphology of MDA-MB-231 or SUM159 cells after FRA1 knockdown for 10 days. Scale bar: 40 μm.

(B) Quantitative PCR for gene expression of mesenchymal markers in FRA1-depleted cells. * denotes significantly different from Luc sh.

(C) Quantitative PCR for gene expression of *FOS* and *FOSL1* after FRA1 knockdown in MDA-MB-231 and SUM159 cells.

(D) Assessment of the tumorgenicity of cancer cells following FRA1 knockdown. 1×10^6 MDA-MB-231 or SUM159 cells were implanted subcutaneously into female NOD-SCID mice, tumors were extracted after 4 weeks, and tumor masses were determined. Numbers indicate the frequency of tumor formation. * denotes significantly different from Luc sh-derived tumors.

(E) Changes in gene expression of EMT markers in Twist-ER and Snail-ER cells after the addition of 4-OHT. Cells were exposed to 4-OHT for the duration examined.

(F) Occupancy of Twist and Snail on the *FOSL1* or *FOS* promoter. Binding enrichment was normalized to input DNA and plotted relative to probe 12 (*FOSL1*) or probe 9 (*FOS*).

(G) Effect of Twist and Snail on FRA1-reporter luciferase activity. Firefly luciferase was normalized against SV40-*Renilla*-luciferase transfection control and the values were compared to control Scr sh or vector overexpression. * denotes significantly different from Scr sh or vector control; n=6.

(H) Quantitative PCR for *FOSL1* expression after Twist or Snail knockdown in NAMECs. * denotes significantly different from vector control.

*p<0.05. Data presented as mean ± s.e.m. See also Figure S5.
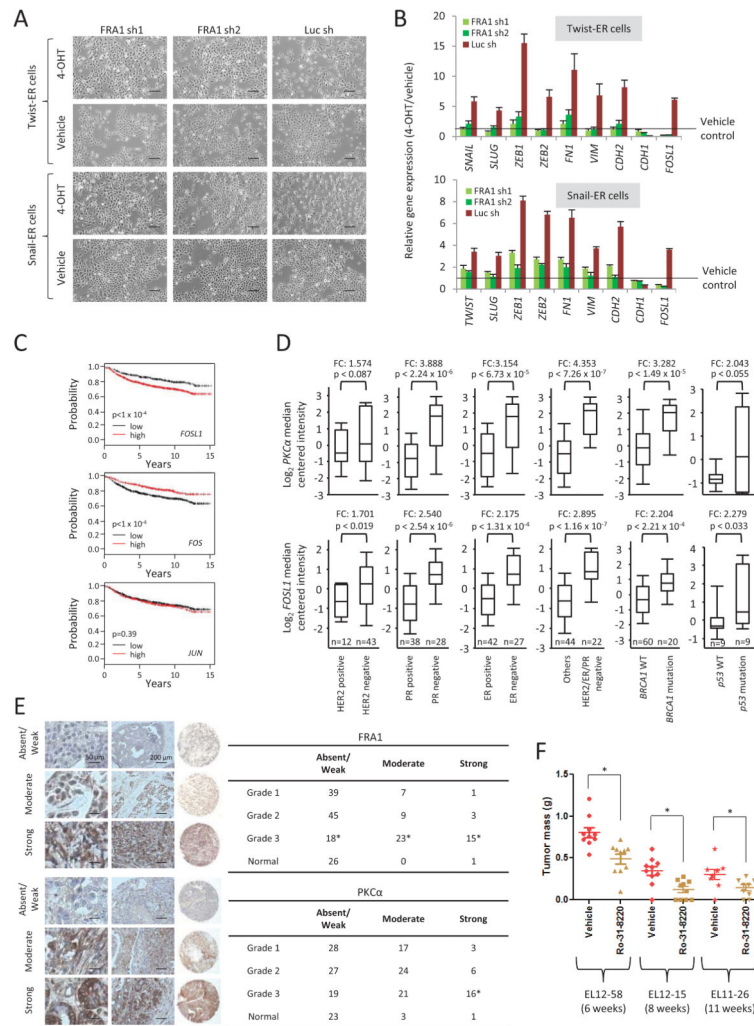
Figure 7. FRA1 is a gatekeeper of the EMT program and is clinically correlated with basal-like or triple-negative breast tumors

(A) Phase contrast images showing morphology of Twist- or Snail-induced EMT cells after FRA1 depletion. Scale bar: 40 μm.

(B) Quantitative PCR for gene expression of EMT-associated mRNAs in Twist-ER and Snail-ER cells following FRA1 knockdown after seven days of 4-OHT exposure.

(C) Kaplan-Meier plots of distant metastasis-free survival of breast cancer patients. Patient groups separated based on *FOSL1* (top), *FOS* (middle) or *JUN* (bottom) mRNA expression.

(D) Microarray meta-analyses of *PKCα* and *FOSL1* mRNA expression in human primary breast cancer tumor subtypes (Waddell et al., 2010), and in breast cancer cell lines bearing *p53* mutation (Neve et al., 2006).

(E) Immunohistochemistry analyses of human breast cancer samples for PKCα and FRA1 protein expression in breast tumors with different grades. Representative staining results are shown at the left. The numbers of graded tumors or normal tissues that were classified based on FRA1 or PKCα expression are depicted at the right. * denotes significantly different from Grade 1, Grade 2 or normal specimens.

(F) Effects of PKCα inhibitor administration (5 mg/kg/day) on the growth of patient-derived breast tumor xenografts in NOD-SCID mice. Treatment was initiated immediately following implantation and continued for five weeks, tumor masses were then determined. * denotes significantly different from vehicle.

*p<0.05. Data presented as mean ± s.e.m. See also Figure S6.
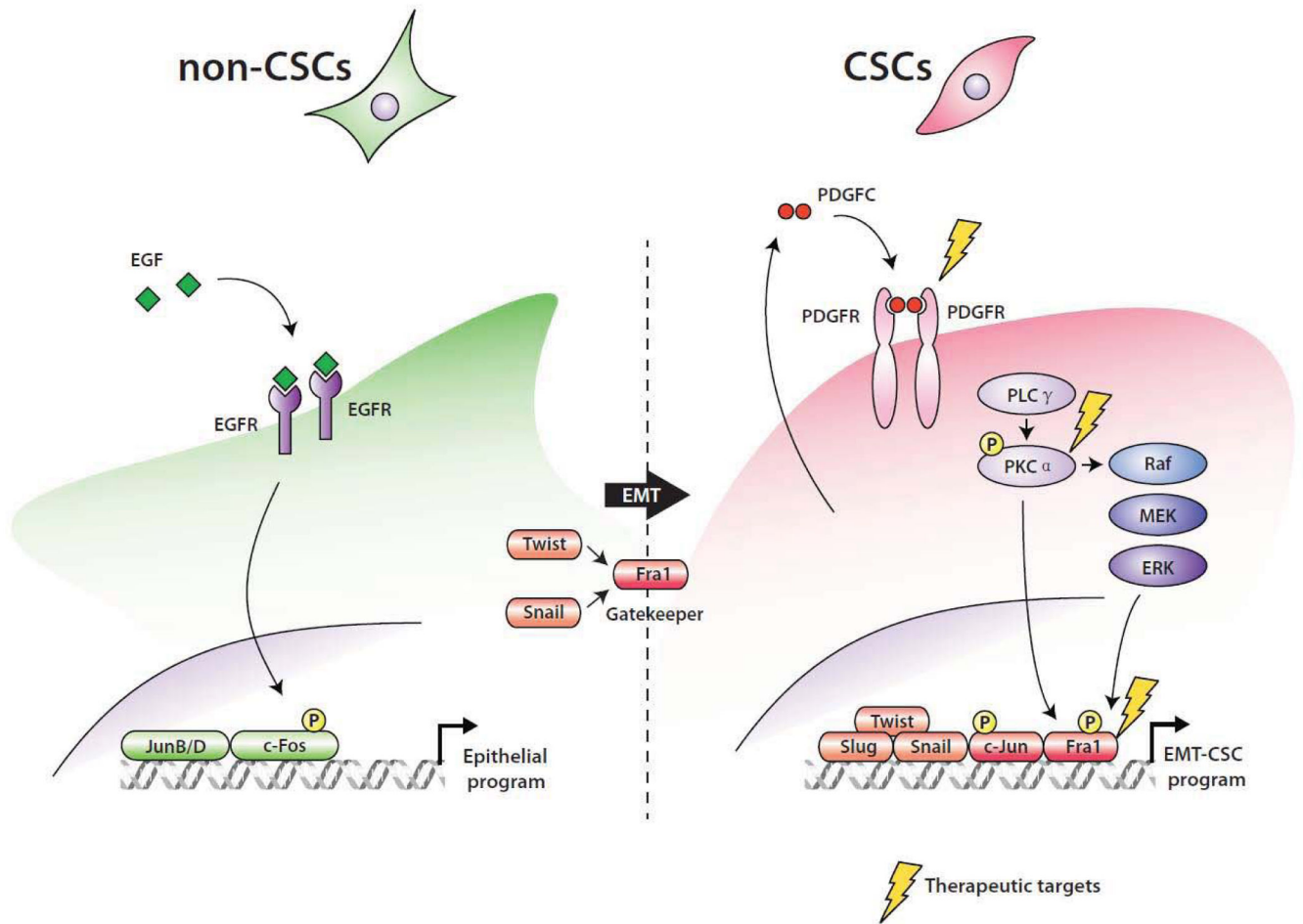
Figure 8.
Scheme depicting the differential utilization of signaling networks between non-CSCs and CSCs upon the activation of an EMT program.